

Synthesis of Block Copolymer Additives for Examining Phase Morphology and
Improving Mechanical Properties of Thermoplastic Elastomers

A Thesis Presented for the
Master of Science
Degree
The University of Tennessee, Knoxville

Bishal S. Upadhyay

December 2023

Copyright © 2023 Bishal S. Upadhyay.
All rights reserved.

ACKNOWLEDGEMENTS

First, I would like to thank Dr. Kilbey for his support and patience throughout my graduate career. His input and guidance have helped me evaluate, learn from my mistakes, and grow as a chemist. I would also like to thank my committee members, Professor Zhao and Professor Heberle, for their insights throughout my graduate career.

I offer a huge, huge thank you to the Kilbey lab members from the past. I thank Sina Sabury for his assistance in synthesis, William Ledford for his “let’s get it done” mentality during early morning lab days, and Elizabeth O’Connell for her in-depth insights into mechanisms and expert NMR interpretations. I would also like to thank the present Kilbey group members, Dani, Nia, Candice, Abby, KJ, and Evan, for all the fun and laughter we have shared, and for their help throughout my time at UTK.

I would also like to thank Dr. Stein and Dr. Karthika Madathil for their help and insights on film formation and SAXS data interpretation. I thank the National Science Foundation for funding the project (Award # DMR-1905487) that supported my work. Finally, I thank you, Mom, and miss you, Dad.

ABSTRACT

Polystyrene-block-poly(1,4-butadiene)-block-polystyrene (PS-PB-PS) triblock copolymers are one of the most widely studied thermoplastic elastomers (TPEs) due to their ease of synthesis, non-polar nature, and commercial applicability. Like many block copolymers, incompatibility between PS and PB causes these TPEs to undergo microphase segregation. Many studies have examined the mechanical properties of blends of TPEs and PS homopolymer additives. However, there have been few studies focused on understanding the morphology and mechanical properties of blends of TPEs and copolymer additives with different architectures. Herein, I describe the synthesis of linear and graft copolymer additives based on the random copolymers poly(methyl methacrylate-random-cyclohexyl methacrylate) (PrC). These copolymers offer composition-tuned miscibility with PS domains of PS-PB-PS TPEs, allowing their enthalpic and entropic effects on morphology, thermal properties, such as glass transition temperature (T_g), and mechanical properties, such as tensile and creep behaviors, to be studied.

TABLE OF CONTENTS

CHAPTER ONE MOTIVIATION AND BACKGROUND	1
1.1 Motivation and Goals.....	1
1.2 Thermoplastic Elastomers.....	4
1.3 Diblock and Triblock Copolymer Systems.....	5
1.4 Controlled Radical Polymerization Techniques: RAFT and ATRP.....	9
1.5 Film Formation	13
1.6 Thesis Organization	14
CHAPTER TWO MATERIALS AND METHODS	15
2.1 Br-PPO Macroinitiator Synthesis	15
2.2 Polymerization using Br-PPO as a Macroinitiator.....	16
2.3 Synthesis of Azido-Functionalized Polymers.....	17
2.4 Synthesis of 2-Bromo-2-Methyl-N-(prop-2-yn-1-yl) Propenamide (BMPP).....	17
2.5 Side Chain Synthesis via BMPP as a Macroinitiator (PrC-BMPP).....	18
2.6 PPO-Based Brush-Like Copolymer Synthesis via Click Chemistry	19
2.7 Linear Copolymer (PrC) Synthesis	20
CHAPTER THREE RESULTS AND DISCUSSION	22
CHAPTER FOUR CONCLUSIONS AND RECOMMENDATIONS	41
LIST OF REFERENCES	43
VITA	45

LIST OF TABLES

Table 3.1: Macromolecular characteristics of PrC copolymers at $f = 0.70$	23
Table 3.2: Macromolecular characteristics of PrC copolymers at $f = 0.30$	29
Table 3.3: Macromolecular characteristics of PrC copolymers at $f = 0.50$	29
Table 3.4: Characteristics of Br-PPO macroinitiator.	32
Table 3.5: Analysis of comb-like copolymers utilizing PPOs of various bromination percentages.	36

LIST OF FIGURES

Figure 1.1:	General design of the PrC additives to be studied in this research.	3
Figure 1.2:	Schematic drawing of phase separated PS-PB-PS triblocks. PS blocks segregate into spherical domains within the matrix, acting as reinforcement for the domains formed by the rubbery PB blocks. PB blocks are denoted by the arrow at the top right of the figure.	6
Figure 1.3:	Diblock copolymer phase diagram showing different morphologies. The horizontal line within the ordered regions indicates order-order phase transitions. The vertical line crossing the boundaries that define the phase envelope traces through several order-disorder transition.	8
Figure 1.4:	Second virial coefficient values describing enthalpic interaction of CHMA/MMA copolymers with PS. The strongest attractive interaction is seen at CHMA composition of 0.7.	11
Figure 1.5:	Design of the low and high molecular weight linear additives incorporated into the TPE matrix where the end blue blocks denote hard PS segments and middle orange block denotes soft PB segment. The black lines denote additive incorporation within the PS blocks of the TPE.	11
Figure 1.6:	Schematic representation of ATRP.	11
Figure 3.1:	Stacked ^1H NMR spectra of PrC copolymers, (Samples 1-5) arranged such that molecular weight increases up the stack consistent with naming in Table 3.1.	25
Figure 3.2:	Stacked ^1H NMR spectra of PrC copolymers, (Samples 6-10) arranged such that molecular weight increases up the stack consistent with naming in Table 3.1.	26
Figure 3.3:	GPC traces of PrC copolymers (Samples 1-5). The legend identifies each PrC by the naming used in Table 3.1.	27
Figure 3.4:	GPC traces of PrC copolymers (Samples 6-10). The legend identifies each PrC by the naming used in Table 3.1.	28
Figure 3.5:	^1H NMR spectrum indicating successful synthesis of Br-PPO.	31
Figure 3.6:	^1H NMR spectrum of PrC brush like copolymer synthesized from a 28% Br-PPO as a macroinitiator. The peak at 3.58 ppm corresponds to the methyl ester of MMA, whereas the peak at 4.56 ppm corresponds to the bridgehead proton of the CHMA.	33
Figure 3.7:	^1H NMR spectrum of PrC brush-like copolymer utilizing 4.5% Br-PPO as macroinitiator. The peak at 3.58 ppm corresponds to the methyl ester of MMA whereas peak at 4.56 ppm corresponds to the bridgehead proton of the CHMA. The peak at 6.47 ppm corresponds to aromatic proton labeled "A" within the structure.	34
Figure 3.8:	^1H NMR spectrum of 2-bromo-2-methyl-N-(prop-2-yn-1-yl) propenamide (BMPP), which is an initiator used to synthesize alkyene-terminated PrC copolymer side chain.	37
Figure 3.9:	^1H NMR spectrum of the alkyene-terminated PrC utilizing BMPP as an initiator for the successful synthesis of 15.4 kDa side chains. The peak at 2.26 ppm confirms the presence of the terminal alkyene used for click reactions between azide groups on the azide-functionalized PPO.	38

Figure 3.10: GPC chromatogram indicating successful synthesis of alkyene-terminated PrC copolymer side chain using BMPP as a macroinitiator. 39

LIST OF SCHEMES

Scheme 2.1: Synthetic scheme for conversion of PPO into Br-PPO.	15
Scheme 2.2: Synthetic scheme for polymerization of Br-PPO-PrC brush-like copolymers utilizing Br-PPO as a macroinitiator at various bromination levels.	17
Scheme 2.3: Synthetic scheme for conversion of Br-PPO to azide-functionalized PPO, which is referred to as PPO-N ₃	17
Scheme 2.4: Synthetic scheme for synthesis of 2-bromo-2-methyl-N-(prop-2-yn-1-yl) propenamide (BMPP).	18
Scheme 2.5: Synthetic scheme for the synthesis of linear random copolymer additives via RAFT polymerization.	21

CHAPTER ONE

MOTIVATION AND BACKGROUND

1.1 Motivation and Goals

Polystyrene-block-poly(1,4-butadiene)-block-polystyrene (PS-PB-PS) triblock copolymers are one of the most widely studied thermoplastic elastomers (TPEs) due to their ease of synthesis, non-polar nature, and commercial applicability.¹ Like many block copolymers, incompatibility between PS and PB causes these TPEs to undergo microphase segregation. Many studies have examined the mechanical properties of blends consisting of TPEs and linear homopolymer additives.² However, there have been few studies focused on understanding the morphology and mechanical properties of blends of TPEs with polymeric additives of different architecture. To enable these studies and as described in this thesis, my goal was to synthesize linear and graft-type copolymeric additives based on methyl methacrylate (MMA) and cyclohexyl methacrylate (CHMA). These comonomers are chosen because varying the molar composition of CHMA in p(MMA-r-CHMA) (PrC) copolymers allows the strength of the enthalpic interaction that drives miscibility with PS to be tuned.³

PS-PB-PS triblocks blended with copolymer additives of different architecture have attracted interest due to major advances in commercial application of TPEs through changes to the block copolymer architecture.⁴ The miscibility of PrC with PS makes this system an ideal candidate for understanding how inclusion and design of the additive affects the mechanical properties and phase behavior of the TPEs. The strength of the enthalpic interaction between PS and PrC can be tuned by changing the composition of CHMA within the PrC.⁵ Entropic effects that affect organization of the additive in PS

domains can be tuned by altering the architecture of PrC. Tuning these attractive enthalpic and entropic interactions of the additive with the PS matrix and examining the morphology will help understand the effect of additive design on properties such as tensile strength, Young's modulus, storage and loss moduli, and creep resistance of TPEs. My thesis research focuses on the synthesis and characterization of the enthalpically-and entropically-tuned copolymer additives. Success with this initiative will enable studies of structure (morphology and phase behavior) and mechanical properties of thermoplastic PS-PB-PS triblock copolymers containing the PrC additives. The additive designs I pursued are pictured in **Figure 1.1**. Herein, I focus on studies that will generate linear copolymer additives of PrC with systematic variations in CHMA composition and chain size. Studies of mechanical properties and morphology of TPEs blended with these linear copolymers were completed by a collaborator.⁶ I also aim to synthesize branched *comb-like* PrC copolymers that can be used as additives with a focus on varying the side chain density. This will ultimately enable studies that address the effect of design on mechanical properties and morphology of TPEs based on PS-PB-PS triblock copolymers. Side chain density brings in entropic effects between the additive and the PS domains formed by microphase segregation of the linear TPE. Given this general overview of my research, the following sections provide relevant background on TPEs, general considerations of phase behavior, atom transfer radical polymerization, which was a key tool used in my research efforts, and aspects of film formation.

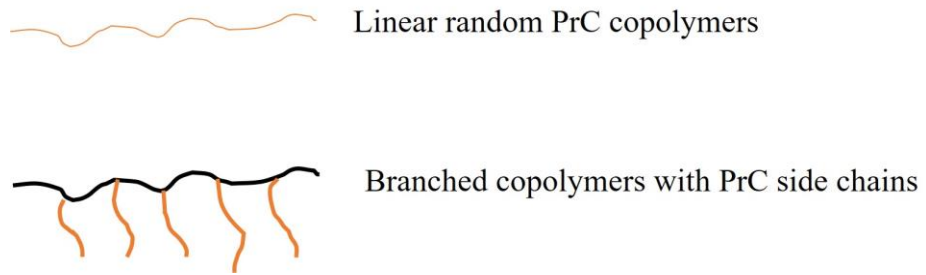


Figure 1.1: General design of the PrC additives to be studied in this research.

1.2 Thermoplastic Elastomers

Thermoplastic elastomers (TPEs) are triblock copolymer systems that have been extensively studied as structural materials and for applications such as sensors, ion-exchange membranes, footwear, vehicle interiors, consumer sporting goods, and fuel cells.⁷ The global demand for TPEs as of 2013 is $\sim 4.5 \times 10^6$ metric tons/year, and applications for motor vehicles represent $\sim 33\%$ of the total consumption.⁸ TPEs are widely used because they possess shorter processing times, can be re-molded, and structures are created by simpler processing steps as compared to traditional thermosets.⁸ Since TPEs are thermoplastics, these elastomers can be processed from solution or thermoformed from the melt state, which decreases the cost of the finished part and enables reprocessing to create new structures that provide properties similar to the original product.⁸

Because they are block copolymers, thermoplastic elastomers undergo microphase separation, segregating into domains that are “hard” at room temperature and domains that are “soft” or rubbery. The classic example of a TPE is a microphase separated A-B-A triblock copolymer, which forms hard domains of polymer A that are dispersed in the soft matrix of polymer B. The hard domains act to stabilize the “network” of flexible domains. The most common examples of A-B-A triblock TPE systems are poly(styrene-*b*-isoprene-*b*-styrene) (SIS) or poly(styrene-*b*-butadiene-*b*-styrene) (SBS).⁹ These TPEs are thermally processable because the glass transition temperature (T_g) of PS is within normal processing ranges (~ 110 °C). The soft blocks have much lower T_g values compared to PS: the T_g of PB and PI are -50 and -60 °C respectively.¹⁰ Therefore, in these triblock copolymers, the hard domains function as a physical crosslinks for the

elastomeric PB (or PI) domains, which provides excellent flexibility and elasticity to the system.⁹ This morphology is shown in **Figure 1.2**. The mechanical properties of these systems are largely influenced by the extent microphase of separation. Lilanonitkul et al.¹¹ showed that the extent of microphase separation could be increased by increasing the hard block sizes via chain extension or by increasing the molecular weight of the soft segments. Elabd et al.¹² studied the use of sulfonated p(styrene-isobutylene-styrene) P(PS-IB-PS) triblock copolymers as ion-exchange resins. In these A-B-A triblock copolymers, the B blocks form bridges and loops, whereas an A-B diblock copolymer, the microphase separated domains lack any bridging or looped chains.¹³ Solution casting was utilized for film formation, and they noticed a significant increase in ion transport properties when the solvent used for drop casting was changed from toluene to a toluene/ethanol mixture, which suggests that the domain structures also depend on the processes used for film formation. Reineke et al.¹⁴ studied the incorporation of sugar-based glassy components in TPEs, and they observed an increase in adhesion and mechanical properties within the biobased TPEs compared to systems with PS end blocks. These studies show that the chemical identity of the blocks impacts properties.

1.3 Diblock and Triblock Copolymer Systems

Diblock copolymers (A-B) are systems in which two homopolymers are connected at a single point. These copolymer types are one of the most widely studied because they are the simplest block copolymer architecture. Many theoretical and experimental studies have been performed to understand the phase behaviors of these systems.³ Diblock copolymers tend to self-assemble into a variety of ordered structures due to the immiscibility of the two blocks due to repulsive enthalpic interactions.^{7, 15} The propensity

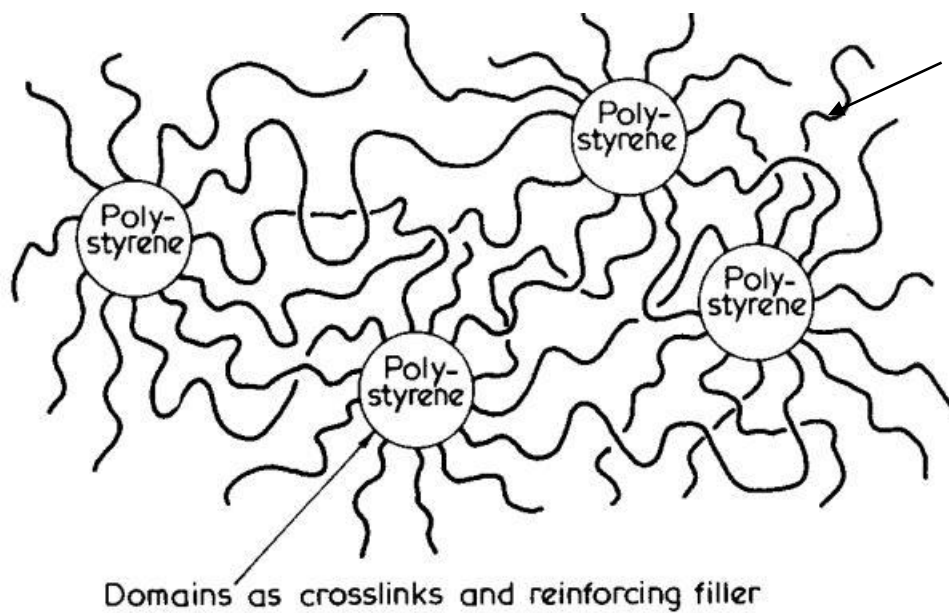


Figure 1.2: Schematic drawing of phase separated PS-PB-PS triblocks. PS blocks segregate into spherical domains within the matrix, acting as reinforcement for the domains formed by the rubbery PB blocks. PB blocks are denoted by the arrow at the top right of the figure. Taken from ref.17.

of immiscible block copolymers to phase separate into microdomains is determined by χN , which is the total enthalpic contribution, where χ is the fundamental pair-wise interaction strength and N is the number of those fundamental interactions between statistical segments on each diblock chain.² The transition from a homogenous melt of chains to a heterogenous melt of ordered, microphase-separated domains is known as the ordered-disordered transition. The type of morphology that is formed by the ordered phase is determined by the copolymer composition, f .⁷ In diblock copolymers, the morphology of microdomains include spherical, cylindrical, gyroid and lamellar, depending on the volume fraction of the blocks, as seen in **Figure 1.3**.¹⁵ A lamellar morphology is seen at nearly symmetric compositions ($f = 0.5$) and the other morphologies appear as the composition deviates from $f = 0.5$.¹⁰ Varying the block copolymer composition also shifts the location of the order-disorder phase boundaries and some of the order-order transitions at values of χN near the order-disorder transition.¹⁵ All of these behaviors can be seen in **Figure 1.3**.

Triblock terpolymers are copolymers that connect three distinct homopolymers system by covalent linkages, and these are often represented as A-B-C copolymers. For any sequence of A, B, and C blocks, different morphologies can be observed, depending on the interaction between the three χ parameters (χ_{A-B} , χ_{B-C} and χ_{A-C}) and the composition of the copolymer system.¹⁶ Hence, triblock copolymers show a richer and more complex morphological behavior than a conventional A-B diblock copolymer systems. The most studied type of triblock copolymer are A-B-A triblocks and, in particular, p(PS-PB-PS) A-B-A triblocks due to their large commercial application. Aggarwal et al.¹⁷ studied the properties of p(PS-PB-PS) triblocks, and they were able to

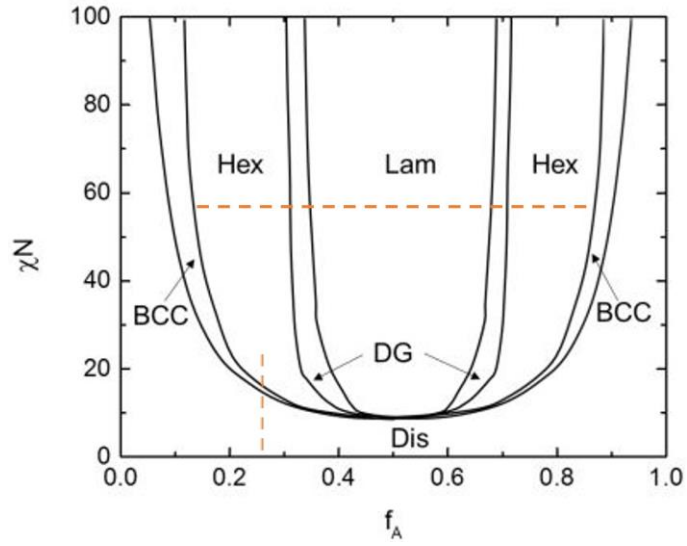


Figure 1.3: Diblock copolymer phase diagram showing different morphologies. The horizontal line within the ordered regions indicates order-order phase transitions. The vertical line crossing the boundaries that define the phase envelope traces through several order-disorder transition. Taken from ref 15.

show that the PS domains segregate as glassy domains, as represented in **Figure 1.2**. As a result, the PS domains act as crosslinks, providing reinforcement to the matrix of PB chains.

Since my thesis work focuses on A-B-A type triblocks, herein I will mostly focus on the morphologies based on these networks. Matsen et al.¹⁵ extensively studied A-B-A triblocks, and they observed the same lamellar, cylindrical, and spherical morphologies as seen in conventional A-B diblock copolymers. Using p(PS-PI-PS) copolymers, Spontak et al.¹⁸ identified the presence of complex gyroid phases on both sides of lamellar region, also suggesting that A-B-A triblocks adopt a similar complex phase behavior as conventional diblock systems. The morphology and phase separation of a diblock system mostly depends on temperature ($\chi \sim 1/T$), composition, and the overall molecular weight of the diblock. The morphologies adopted by triblock copolymers follow the same trend as well.¹⁵ Thus **Figure 1.3** could be viewed as a “classical” phase diagram for A-B-A triblock copolymers.

1.4 Controlled Radical Polymerization Techniques: RAFT and ATRP

Controlled radical polymerizations (CRPs)¹⁹ are one of the most common and widely used synthetic technique due to their robustness, ability to make a variety of desired architectures, and the tolerance to many monomer types, including acrylates, methacrylates, and styrenic monomers. CRP techniques employ a reversible activation/deactivation process, where the dynamic equilibrium between the “dormant” state and “active” state (or the propagating radical) plays a key role in controlling the molecular weight. The most popular CRP methods are reversible addition fragmentation-chain transfer (RAFT) polymerization and atom transfer radical polymerization (ATRP).

Random copolymers of PrC were synthesized via RAFT polymerization using 4-cyano-4-(phenylcarbonothioylthio)pentanoic acid as the chain transfer agent (CTA). The detailed synthesis scheme is discussed in **Chapter 2**. The molecular weight of the PrC additive was controlled by changing the [monomer]: [CTA] ratio, and copolymers with different compositions (f) of CHMA were synthesized at $f = 0.3, 0.5$ and 0.7 . A Flory Huggins analysis of cloud point data shows that these CHMA compositions have an attractive enthalpic interaction with PS.⁵ The composition dependence of the second virial coefficient (B) as a function of molar composition of MMA and CHMA is shown in **Figure 1.4**, and it indicates that there is a favorable interaction with PS when f_{CHMA} ranges from 0.3 to 0.7. The highest interaction strength occurs at $f_{\text{CHMA}} 0.7$ ($\chi \sim -0.02$).⁵ This behavior shows that the strength of the interaction between the PrC copolymer and PS can be tuned by varying the CHMA composition. In the case of the TPEs used in our studies, we believe that PrC copolymer additives with slightly shorter or similar chain lengths to the PS blocks of the TPE will distribute throughout the PS domains, thus increasing the mechanical properties, strength, and creep resistance of the blend. On the other hand, larger copolymer additives will be located towards the center of the PS domains, potentially acting as a bridge between two layers to improve toughness and ductility.¹⁷ In essence, short PrC will mix with PS blocks, but larger PrC chains cannot intermix easily due to their size. These ideas are depicted in **Figure 1.5**.

ATRP is one of the most widely used CRP techniques for the synthesis of linear, branched, and complex star-like polymers. **Figure 1.6** shows a schematic representation of polymer synthesis via ATRP. ATRP allows for the synthesis of well-defined block copolymers with controlled molecular weight and narrow dispersity while allowing for

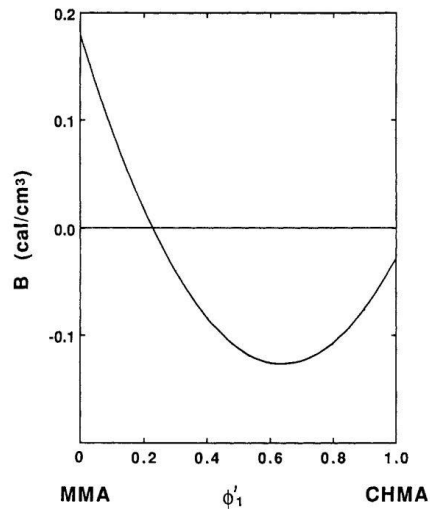


Figure 1.4: Second virial coefficient values describing enthalpic interaction of CHMA/MMA copolymers with PS. The strongest attractive interaction is seen at CHMA composition of 0.7. Taken from ref 5.

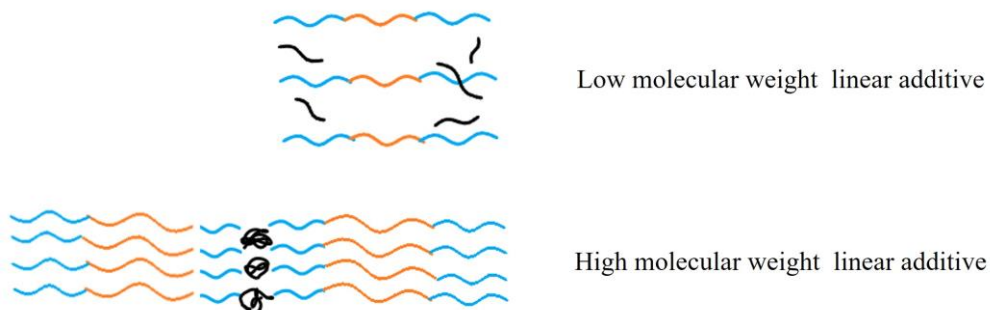


Figure 1.5: Design of the low and high molecular weight linear additives incorporated into the TPE matrix where the end blue blocks denote hard PS segments and middle orange block denotes soft PB segment. The black lines denote additive incorporation within the PS blocks of the TPE.

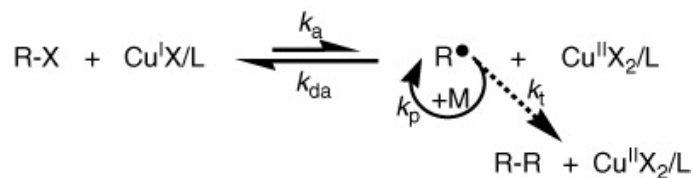


Figure 1.6: Schematic representation of ATRP. Taken from ref 20.

end group functionalization. Different initiator designs enable the synthesis of different molecular architectures.²⁰ New polymeric structures with reactive functional moieties can be synthesized with wide range of applications in mind. ATRP has been utilized often for the synthesis of polymeric molecular brushes.²¹ Molecular polymer brushes are a class of polymeric architecture with dense arrays of side chains. Often, they are synthesized through the use of a functional moiety placed along the chain backbone, enabling side chains to be grown, from less to densely-grafted brushes. Brushes that are synthesized this way are made via “grafting from”, but there are also “grafting through” and “grafting onto” methods. “Grafting from” is a technique where the backbone containing reactive functional moieties is first synthesized. A post-polymerization technique, often utilizing ATRP or RAFT polymerization, is then used to grow side chains from the backbone. “Grafting from” is one of the most widely used techniques and has been considered the most effective and efficient way to synthesize molecular brushes.²² A second method, “grafting through” utilizes low molecular weight macromonomers that are polymerized to create the molecular brush. “Grafting onto” involves attachment of premade, end functionalized chains to a backbone containing a complementary reactive group. High efficiency reactions are needed, so “click” chemistry is often used to synthesize star-like or lightly-grafted brush copolymers.²³

For this project the “grafting from” method was first employed to synthesize polymer brushes. Specifically, a brominated poly(phenylene oxide) or Br-PPO, was used as the macroinitiator for the synthesis of PrC side chains. Poly(phenylene oxide) (PPO) is a commercially available engineering plastic that has a high T_g of 212 °C.²¹ PPO-based additives have been commonly utilized with PS-based block copolymers due to their

miscibility, increased in tensile strength and moduli, and improved thermal stability.²⁴ However, PPO-based systems suffer drawbacks to melt processing due to their higher T_g . PPO is also synthesized by oxidative coupling²⁴ which leads to high dispersity, as discussed later in **Chapter 2**. My grafting from approach using Br-PPO as a macroinitiator was impacted by several issues. Hence, the approach was changed to “grafting onto” method. For this, I synthesized an alkyne terminated ATRP initiator for synthesis of PrC copolymer side chains. After the successful synthesis of various side chains, the alkyne functionalized polymer was grafted onto PPO-N₃ via a click chemistry reaction. This work is described in **Chapter 2**.

1.5 Film Formation

There are several techniques used to deposit thin films on surfaces, including spin casting, flow-coating, and drop casting. In spin casting, a polymer solution is deposited onto a rotating substrate, creating a uniform film due to rapid radial flow and ejection of solution from the substrate edge and solvent evaporation.²⁵ Flow coating of polymer films involves mechanical spreading of a viscous polymer solution onto a solid substrate, for example, by a doctor blade.²⁶ Compared to spin casting, flow coating is less violent and usually requires a less volatile solvent. The drop casting method is an easy and tunable deposition method in which a polymer solution is dispersed over a substrate that is allowed to dry under conditions of controlled pressure and temperature. The film thickness is strongly dependent on the deposition volume and copolymer concentration, which can be easily tuned.²⁸ In all these methods, parameters such as solvent type, copolymer concentration, and temperature affect the deposition process and influence film thickness and morphology.² Once solution deposited or cast, the rate of solvent

evaporation dictates the nature of cast film, making solvent choice a critical parameter in film formation. Highly volatile organic solvents are often chosen because they lead to the near-immediate formation of smooth films while preventing dewetting of the polymer from the substrate.²⁷ Copolymer concentration also plays a key role, as extremely high and low concentrations lead to films of irregular thickness.²⁸ Thin films containing linear copolymer additives incorporated into TPE matrix were prepared by mixing the TPE and the additive at different volume fractions in xylene. The films were prepared by blade coating the polymer solution onto Mylar sheets using an Elcometer film applicator. The films were dried in air then annealed in the vacuum oven for 48 h at 140 °C. After cooling, these films were used for morphological and mechanical studies.⁶

1.6 Thesis Organization

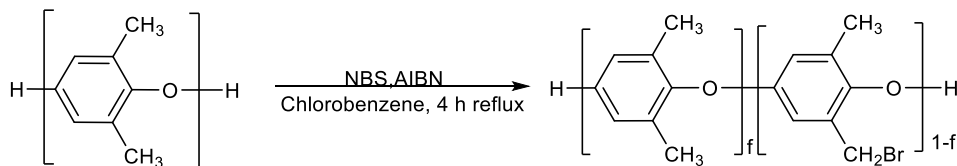
This thesis is organized as follows: **Chapter 2** describes materials and procedures used in this research, including protocols used to synthesize the linear PrC. Also presented are approaches used to create branched copolymers. **Chapter 3** describes the results obtained, along with figures to provide explanation for the synthesis of different compositions of the linear copolymers. The branched copolymers were synthesized via two different ATRP grafting methods due to issues with synthesis, which are discussed in depth. Finally key conclusions and ideas for future work are presented in **Chapter 4**.

CHAPTER TWO

MATERIALS AND METHODS

2.1 Br-PPO Macroinitiator Synthesis

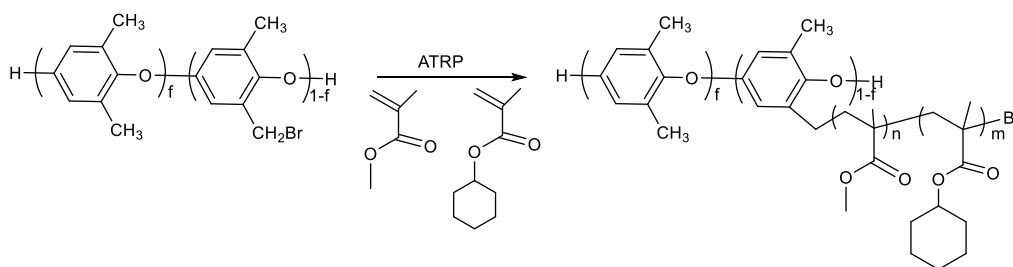
Brominated poly(phenylene oxide) (Br-PPO) was synthesized following protocols detailed in literature²⁸ as shown in **Scheme 2.1**. In short, poly(phenylene oxide) (PPO) (1 g, 0.045 mmol), N-bromo-succinimide (NBS) (0.24 g, 1.35 mmol), 2,2'-Azobis(2-methylpropionitrile) (AIBN) (0.022 g, 0.125 mmol) were dissolved in 13 mL of chlorobenzene and added to a 25 mL round bottom flask equipped with a magnetic stir bar. The flask was fitted with a condenser and immersed in a preheated oil bath set to 135 °C. The reaction flask left to reflux for 4 h. After 4 h, the reaction mixture was precipitated into cold methanol. The product acquired was dried for 24 h and stored under argon prior to use. Characterization by gel permeation chromatography (GPC) showed that the brominated PPO had an $M_n = 29$ kDa and a dispersity $\mathcal{D} = 1.89$. The proton nuclear magnetic resonance (^1H NMR) spectrum, shown in **Chapter 3**, confirmed the formation of Br-PPO, with the peaks at 6.67 and 6.47 ppm corresponding to the aromatic protons and the peak at 4.34 corresponding to benzylic protons.



Scheme 2.1: Synthetic scheme for conversion of PPO into Br-PPO.

2.2 Polymerization using Br-PPO as a Macroinitiator

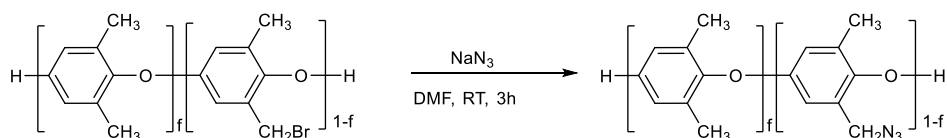
After the successful synthesis and characterization of the Br-PPO macroinitiator, brushes with side chains of different molecular weight were synthesized via ATRP, as shown in **Scheme 2.2**. A typical reaction was formulated such that [M]: [I]: [CuBr]: [Me₆TREN] was 100:1:1:1, which targets 14.6 kDa side chain size. Cu(I)Br (3.707×10⁻⁵ mmol, 5 mg,) was added to a dry scintillation vial and degassed under argon. Subsequently, a mixture of MMA (3.707×10⁻³ mmol, 118 μL), CHMA (3.707×10⁻³ mmol, 452 μL), Me₆-TREN (3.707×10⁻⁵ mmol, 9.46 μL), and 6 mL of benzene were added to the same scintillation vial. The vial was capped and allowed to stir at 300 rpm for 30 min to allow for copper complex formation. In another vial, Br-PPO (3.707×10⁻⁵ mmol, 13.9 mg) was dissolved in 6 mL of benzene for 30 min. A Schlenk flask with a stir bar was flame dried, vacuum evacuated 3× and septum capped. The constituents were then added via syringe under positive argon pressure. Once added, three to four freeze-pump-thaw cycles were used to remove dissolved oxygen. Then, the flask was submersed in an oil bath pre-heated to 70 °C for 6 h. After this time, the polymerization was quenched by submerging the flask into liquid nitrogen and opening it to air. After thawing, the crude product was diluted with THF and passed through a basic alumina column to remove the copper complex. The product was collected and then precipitated in cold methanol and gravity filtered to isolate the final product. The polymer was dried overnight under an active vacuum at room temperature and subsequently characterized via ¹H NMR and GPC.



Scheme 2.2: Synthetic scheme for polymerization of Br-PPO-PrC brush-like copolymers utilizing Br-PPO as a macroinitiator at various bromination levels.

2.3 Synthesis of Azido-Functionalized Polymers

Because of challenges with ATRP using Br-PPO as a macroinitiator in a grafting from approach, azide-functionalized PPOs were synthesized following a procedure detailed in literature.²² In short, the brominated PPO macroinitiator (0.0209 mmol, 390 mg) was reacted with sodium azide (NaN_3) (0.0378 mmol, 2.46 mg) in 7 mL of DMF, as represented in **Scheme 2.3**. After 3 h, the solution was precipitated into cold methanol and gravity filtered to obtain the product. The resulting powder was dried overnight under an active vacuum at room temperature and subsequently characterized via ^1H NMR.

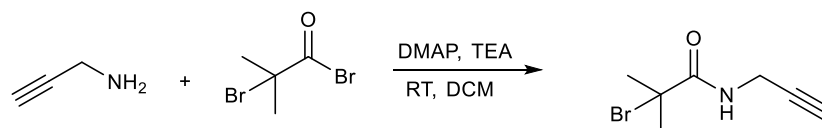


Scheme 2.3: Synthetic scheme for conversion of Br-PPO to azide-functionalized PPO, which is referred to as PPO- N_3 .

2.4 Synthesis of 2-Bromo-2-Methyl-N-(prop-2-yn-1-yl) Propenamide (BMPP)

Due to issues with grafting from using the Br-PPO macroinitiator, a small molecule ATRP initiator that can be used in a grafting-to approach was prepared following a procedure adapted from literature,²⁹ as represented in **Scheme 2.4**. In short, a solution containing propargyl amine (15.6 mmol, 999 μL), 4-dimethyl amino pyridine (DMAP)

(7.8 mmol, 953 mg), and triethylamine (TEA) (23.4 mmol, 3.26 mL) in 30 mL of dry dichloromethane was made in a round bottom flask containing a stir bar. The flask was placed in an ice water bath (0 °C) and stirred for 10 min. In a scintillation vial, a solution of 2-bromoisobutyryl bromide (14.4 mmol, 1.77 mL) in 20 mL dry dichloromethane was prepared and then added dropwise to the round bottom flask. The reaction mixture was stirred overnight at room temperature. The mixture was extracted 3× with a 50:50 DCM/water mixture. The organic phases were combined and dried over MgSO₄ for 10 min. Subsequently, the solids were removed by gravity filtration and the solvent was evaporated utilizing a rotary evaporator. The yellowish product, referred to as BMPP, was purified via column chromatography using a 1:1 ethyl acetate: hexane solvent system. ¹H NMR (500MHz, CDCl₃): 4.06 (m, CH-C-CH₂), 2.27 (t, CH-C), 1.9 (s, C-(CH₃)₂Br), 7.03 (s, 1H, NH). (See **Chapter 3** for the ¹H NMR spectrum.)



Scheme 2.4: Scheme for synthesis of 2-bromo-2-methyl-N-(prop-2-yn-1-yl) propenamide (BMPP).

2.5 Side Chain Synthesis via BMPP as a Macroinitiator (PrC-BMPP)

After the successful synthesis and characterization of the BMPP initiator, PrC side chains of different molecular weight were synthesized via ATRP. For these polymerizations, ratios of [M]: [I]: [CuBr]: [Me₆TREN] of 100:1:1:1 were used to target a side chain size of 14.6kDa. Cu(I)Br (7.415×10⁻⁵ mol, 10.48 mg), CHMA (3.707×10⁻³ mol, 987 μL), MMA (3.707×10⁻³ mol, 387 μL), and Me₆TREN (7.415×10⁻⁵ mol, 19 μL) were added to a 50 mL Schlenk flask equipped with a magnetic stir bar. The reaction

mixture was degassed by 3 successive freeze-pump-thaw cycles. After the last cycle, the vessel was purged with argon and then allowed to react for 6 h in a hot oil bath pre-set at 70 °C. The reaction was quenched by opening the flask to air and diluting the contents with THF. Then, the diluted mixture was passed through a basic alumina column to remove the copper catalyst complex. After its removal, THF was removed using rotary evaporation at reduced pressure, and the polymer was then precipitated into cold methanol. The product was collected by gravity filtration and dried overnight under an active vacuum at room temperature. The PrC side chain copolymers obtained were analyzed via ¹H NMR and discussed in-depth in **Chapter 3**.

2.6 PPO-Based Brush-Like Copolymer Synthesis via Click Chemistry

For the synthesis of molecular brushes consisting of PPO backbones and PrC side chains, click chemistry was utilized. The procedure was adapted from literature.³⁰ In a vial, Cu(I)Br (22 mg, 158 mmol), PMDETA (33 μL, 158 mmol) and azide-terminated PPO (PPO-N₃) (118 mg, 264 mmol) in 3 mL of THF were combined and stirred for 45 min until the solution turned bright green. In a separate vial, PrC-BMPP (30 mg, 135 mmol) was dissolved in 1.35 mL of dry THF. The contents of the two separate vials were added to a 50 mL Schlenk flask under argon and subjected to three freeze-pump-thaw cycles. After the completion of the third cycle, the flask was placed in an oil bath pre-set to 40 °C and stirred for 14 h. The reaction was quenched by opening the flask to air and diluting the contents with THF. Then, the diluted mixture was passed through a basic alumina column to remove the copper catalyst complex. After removal of the copper complex, THF was removed using rotary evaporation at reduced pressure, and the

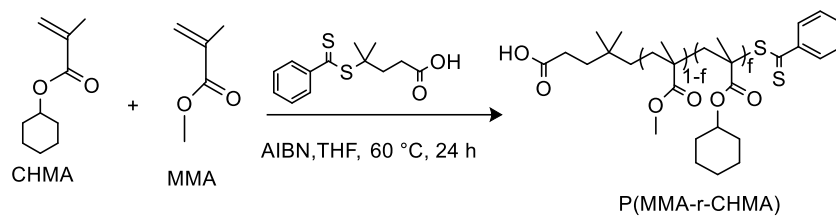
polymer was then precipitated into cold methanol. The final product was collected by gravity filtration and dried overnight under a dynamic vacuum at room temperature.

2.7 Linear Copolymer (PrC) Synthesis

Linear copolymers resulting from random incorporation of cyclohexyl methacrylate (CHMA) and methyl methacrylate (MMA) were synthesized via reversible addition-fragmentation chain transfer (RAFT) polymerization, as seen in **Scheme 2.5**. The strategy adapts procedures described previously.³¹ For all RAFT polymerizations, the target copolymer composition was fixed at 70 mol% of CHMA, as it is reported to result in the minimum χ parameter when blended with polystyrene.⁵ Copolymer molecular weight was varied by changing the total monomer concentration, and at higher molecular weights, the feed ratio of CHMA:MMA had to be adjusted to hit the target composition.

As an example, CHMA (64.4 mmol, 10.82 g), MMA (27.6 mmol, 2.76 g), 4-cyano-4-(phenylcarbonothioylthio)pentanoic acid (1 mmol, 279 mg), and AIBN (0.1 mmol, 16.8 mg) were dissolved in 10 mL of THF and added to 25 mL round bottom flask equipped with a stir bar. The flask was sealed with a septum and dissolved oxygen removed through three freeze-pump-thaw cycles. The flask was then immersed in a preheated oil bath set to 70 °C. After 18 h, the reaction was quenched by opening the flask to air and freezing the crude product mixture with liquid nitrogen. After thawing, the copolymer was isolated and purified by precipitation into cold methanol and gravity filtration. The recovered PrC copolymer was dried under vacuum for 24 h prior to use. Characterization by GPC and NMR spectroscopy showed that this PrC had an $M_n = 2,800$ g/mol, a

dispersity $\mathcal{D} = 1.09$, and a mole fraction of CHMA, $f_{\text{CHMA}} = 0.72$. The characteristics of all PrCs synthesized are discussed in-depth in **Chapter 3**.



Scheme 2.5: Scheme used for the synthesis of linear random copolymer additives via RAFT polymerization.

CHAPTER THREE

RESULTS AND DISCUSSION

3.1 Linear Copolymers (PrCs)

As previously discussed, PrCs are random copolymers that exhibit miscibility with PS domains within SEBS, resulting in changes in morphology and in thermal and mechanical properties. Therefore, changing the composition and molecular weight of the PrC can further tune these properties. Specifically, linear block copolymers of PrC have been proven to be miscible with PS homopolymers at molar CHMA compositions ranging from 0.3 to 1.0.⁵ However, the miscibility of CHMA-based copolymers with PS-containing TPE has not been explored. It is anticipated that the PrC will be miscible with PS domains of TPEs. To understand this further, I synthesized various linear copolymers having molar CHMA compositions of 0.3, 0.5 and 0.7. The effect of PrC composition on miscibility of PS is shown in **Chapter 1**, where the maximum miscibility of the copolymer additive occurs at a CHMA composition of 0.7. With this basis, I was able to synthesize samples ranging from 2.4 kDa to 65.3 kDa. The complete set of data is seen in **Table 3.1**. I was able to synthesize low and high molecular weight copolymers at the desired compositions. However, it was observed that with increasing molecular weight, the composition of the copolymer varied from the comonomer feed ratio because the random copolymers were enriched in CHMA. To tackle this issue, the comonomer feed ratio was adjusted to 75:25 CHMA: MMA, which allowed to effectively achieve 0.7 molar composition of CHMA at higher molecular weight samples.

¹H NMR was used to determine the PrC copolymer composition. Copolymer composition was calculated from integrated peak areas corresponding to the methyl ester

Table 3.1. Macromolecular characteristics of PrC copolymers at $f = 0.70$.

Sample	CHMA: MMA (mmol) ^a	Mol Fraction of CHMA ^b	Mol Fraction of MMA ^b	f_{CHMA} ^c	M_n ^d (kg/ mol)	\bar{D}	N_{MMA} ^e	N_{CHMA} ^e
Sample 1	13.3: 5.70	0.70	0.30	0.72	2.8	1.09	5	14
Sample 2	21.0: 9.0	0.70	0.30	0.73	4.4	1.08	8	22
Sample 3	8.81: 2.95	0.75	0.25	0.76	10	1.13	17	52
Sample 4	19.9: 8.59	0.70	0.30	0.74	12.5	1.12	23	61
Sample 5	15.0: 5.0	0.75	0.25	0.78	17	1.13	25	86
Sample 6	87.5: 37.5	0.70	0.30	0.75	18.5	1.13	33	91
Sample 7	18.8: 6.25	0.75	0.25	0.75	21.2	1.14	35	106
Sample 8	25.3: 8.45	0.75	0.25	0.76	28.5	1.06	45	143
Sample 9	28.6: 19.0	0.60	0.39	0.66	34.8	1.16	81	159
Sample 10	58.2: 19.4	0.75	0.25	0.76	65.5	1.11	103	329

^a ratio of monomers in feed. ^b mole fraction of CHMA and MMA in solution. ^c mole fraction CHMA in copolymer, as determined from ¹H NMR. ^d number-average molecular weight determined by GPC (relative to PS standards). ^e number of repeats units of each comonomer based on M_n .

of the MMA (at 3.57-3.58 ppm; labeled “a” on **Figure 3.1** and **3.2**) and the proton at the bridgehead position of CHMA (at 4.63-4.65 ppm; labeled “b” on **Figure 3.1** and **3.2**). Spectra were acquired in CDCl₃, as evidenced by the residual solvent peak at 7.26 ppm. GPC measurements were performed on all the samples to assess their molecular weight and dispersity. The stacked GPC chromatograms are shown in **Figure 3.3** for samples 1 through 5 and in **Figure 3.4** for samples 6 through 10, respectively. After the successful synthesis and characterization, blends were prepared by mixing TPE and the PrC additive at 10 wt% then cast onto Kapton sheets. The resulting films were used to examine the morphology. Young’s modulus, yield stress, toughness and creep measurements were performed on these linear blend systems by a collaborator.⁶

Linear copolymers at CHMA composition of 0.3 and 0.5 were also synthesized following the exact procedure and characterization methods described above. The target molecular weights for CHMA composition of 0.3 and 0.5 is seen in **Table 3.2** and **Table 3.3**, the target molecular weights for those systems were identical to the samples listed in **Table 3.1**. However, because the enthalpic driving force for miscibility of the additives within the PS domain of the SEBS is maximized at CHMA molar composition of 0.7, only those samples were extensively characterized and studied. Future efforts may involve studying the effects of these PrC with lower CHMA content on morphology and properties of TPEs.

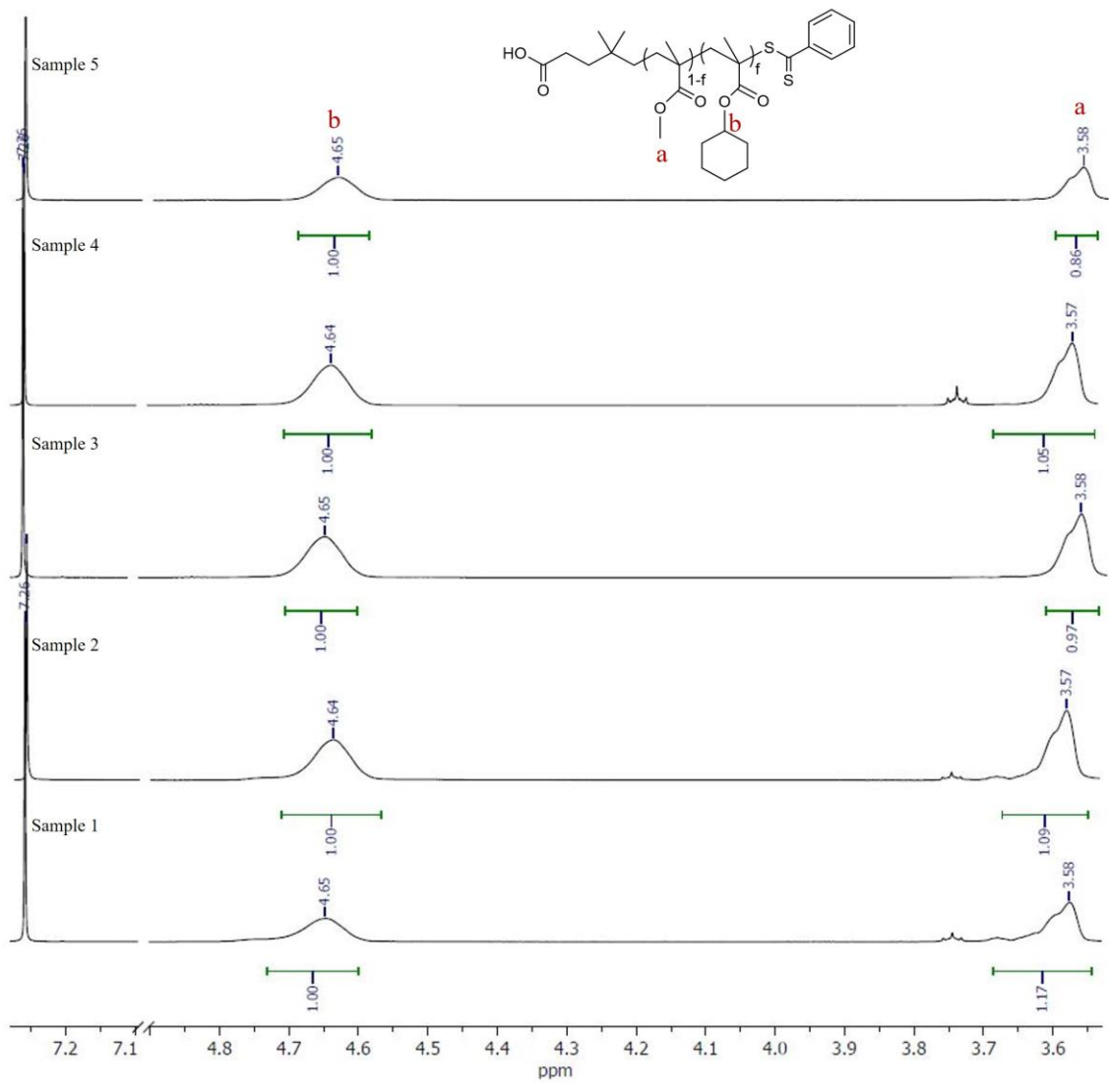


Figure 3.1: Stacked ¹H NMR spectra of PrC copolymers, (Samples 1-5) arranged such that molecular weight increases up the stack consistent with naming in **Table 3.1**.

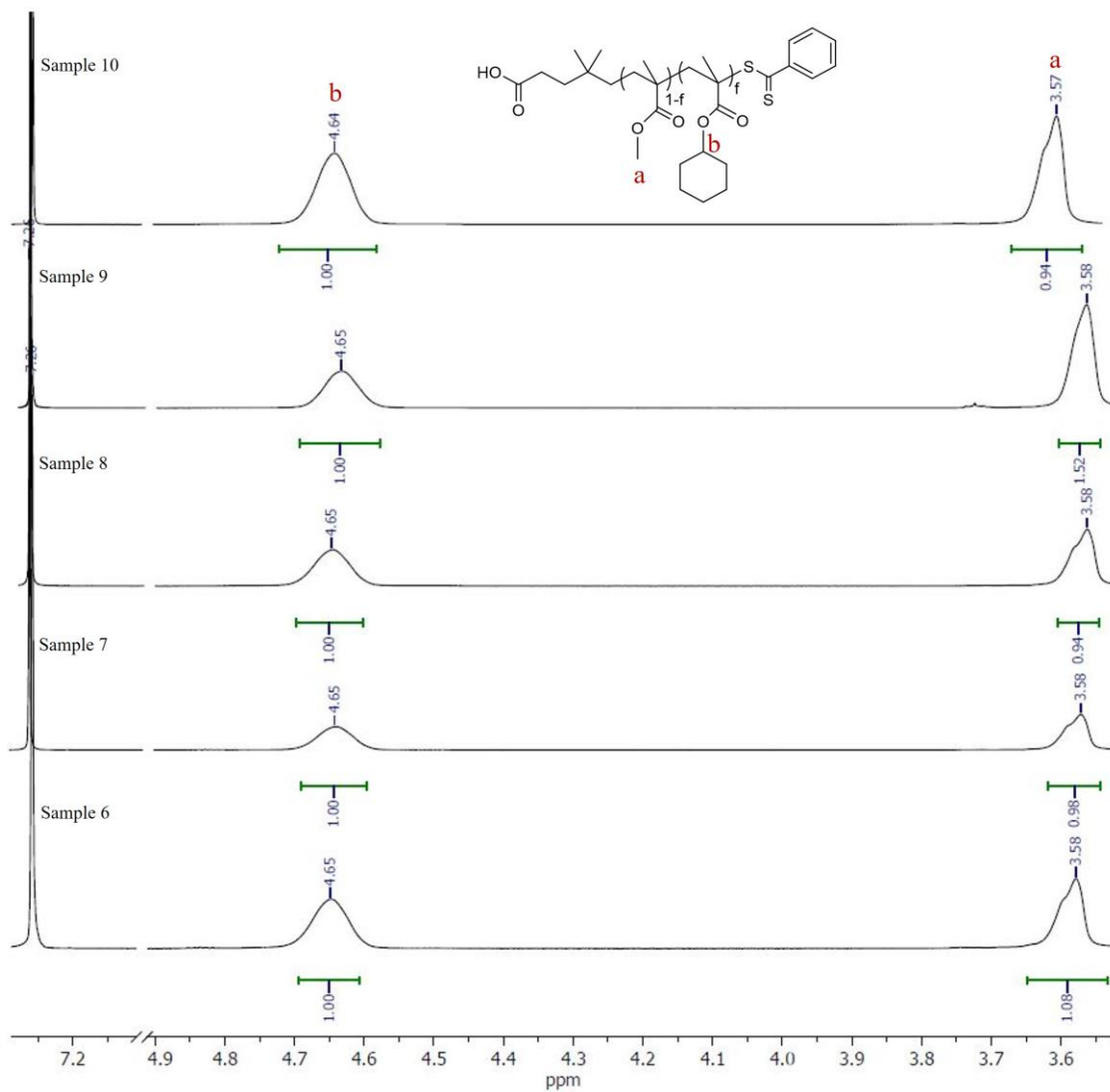


Figure 3.2: Stacked ¹H NMR spectra of PrC copolymers, (Samples 6-10) arranged such that molecular weight increases up the stack consistent with naming in **Table 3.1**.

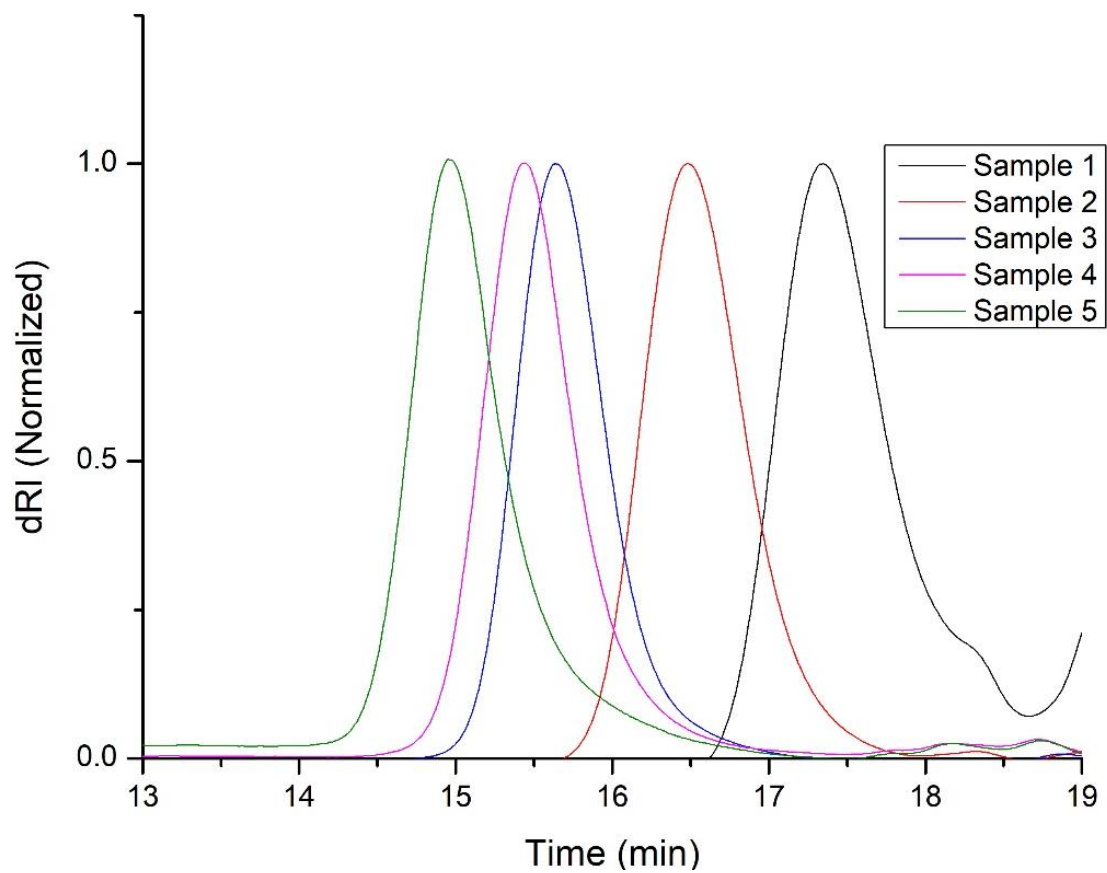


Figure 3.3: GPC traces of PrC copolymers (Samples 1-5). The legend identifies each PrC by the naming used in **Table 3.1**.

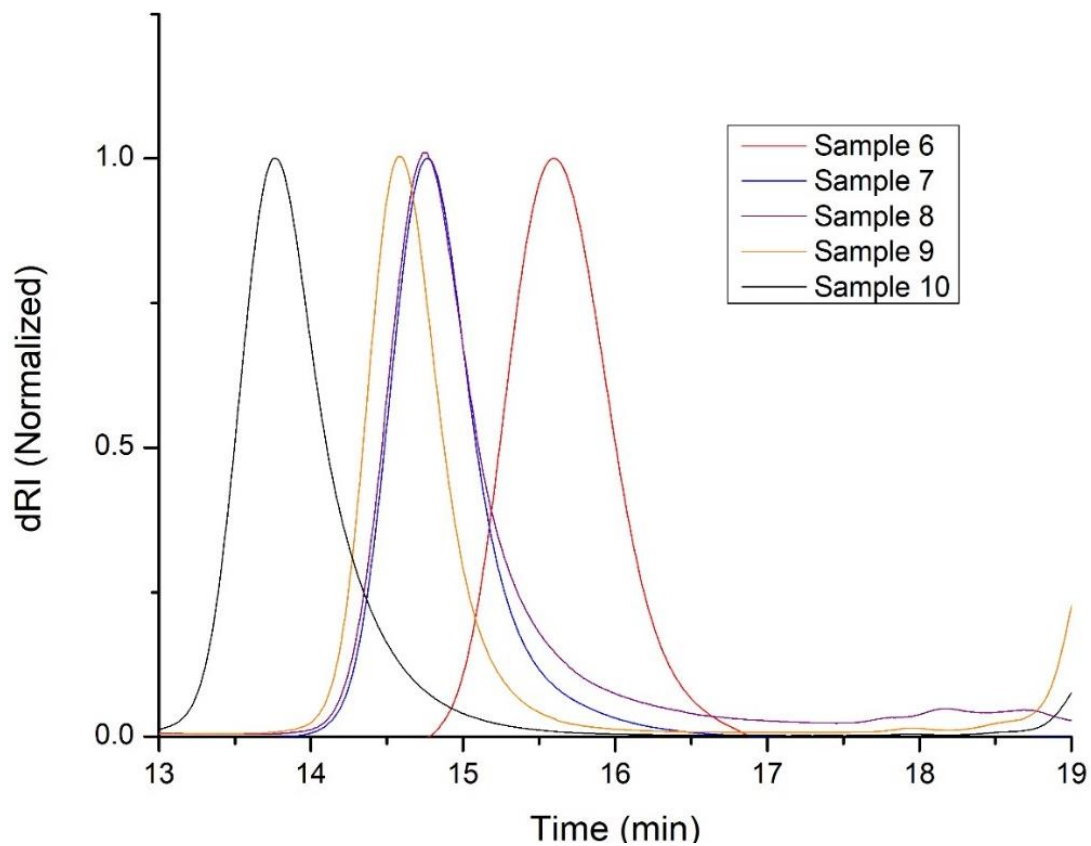


Figure 3.4: GPC traces of PrC copolymers (Samples 6-10). The legend identifies each PrC by the naming used in **Table 3.1**

Table 3.2. Macromolecular characteristics of PrC copolymers at $f = 0.30$.

Sample	M_n (kg/mol) ^a	\bar{D}	f_{CHMA} ^b	N_{MMA} ^c	N_{CHMA} ^c
Sample 11	1.60	1.12	0.32	9	4
Sample 12	4.50	1.11	0.36	13	23
Sample 13	10.0	1.08	0.43	47	36
Sample 14	23.0	1.09	0.35	117	71
Sample 15	30.0	1.15	0.34	161	83

^a number-average molecular weight determined by GPC (relative to PS standards). ^b mole fraction CHMA in copolymer, as determined from ¹H NMR. ^c number of repeats units of each comonomer based on M_n .

Table 3.3. Macromolecular characteristics of PrC copolymers at $f = 0.50$.

Sample	M_n (kg/mol) ^a	\bar{D}	f_{CHMA} ^b	N_{MMA} ^c	N_{CHMA} ^c
Sample 16	2.70	1.05	0.59	8	12
Sample 17	5.20	1.11	0.58	15	22
Sample 18	11.0	1.08	0.53	39	45
Sample 19	20.0	1.06	0.52	70	78
Sample 20	30.7	1.12	0.52	110	118

^a number-average molecular weight determined by GPC (relative to PS standards). ^b mole fraction CHMA in copolymer, as determined from ¹H NMR. ^c number of repeats units of each comonomer based on M_n .

3.2 Branched Copolymers

The structure of a branched PrC copolymer utilizing Br-PPO as a macroinitiator was synthesized. The percent bromination was controlled by tuning reaction time. I targeted 5%, 10% and, 25% bromination levels. **Figure 3.5** presents a ^1H NMR spectrum of a successful synthesis of Br-PPO at 4.5% bromination, which I was able to obtain at a high yield of 88%. No bromination of the phenyl ring was observed.²¹ I used ATRP to grow PrC side chains utilizing benzene as a solvent. **Table 3.4** summarizes the characteristics of the Br-PPO macroinitiator. The Cu(I)-Br/Me₆TREN catalyst complex was chosen for these polymerizations, as it shows faster initiation of the benzylic halide (bromine), thus prompting comparatively shorter reaction times. Other metal ligand systems, such as Cu(I)-Br/PMDETA, were also attempted, but this complex showed no activation of the macroinitiator. **Figure 3.6** shows the ^1H NMR spectrum of a brush-like copolymer that was created from a Br-PPO with 27 Br sites along the backbone. The spectrum shows that the CHMA:MMA copolymer composition is 73:27. The GPC elugram shows a $M_n = 3.07 \times 10^3$ kDa, which is three times higher than the target $M_n = 1.07 \times 10^3$ kDa. This likely indicates crosslinking of the side chains or potential crosslinking of the PPO backbone. In fact, for some Br-PPO systems with higher initiator sites, a complete gel-like product was acquired, which hindered or prevented further characterization.

To further understand this suspicion, I used the 4.5% brominated PPO to perform the polymerization. **Figure 3.7** shows the ^1H NMR spectra of the resulting copolymer, which shows a CHMA:MMA ratio of 72:28. In this synthesis, methyl protons of the Br-PPO are

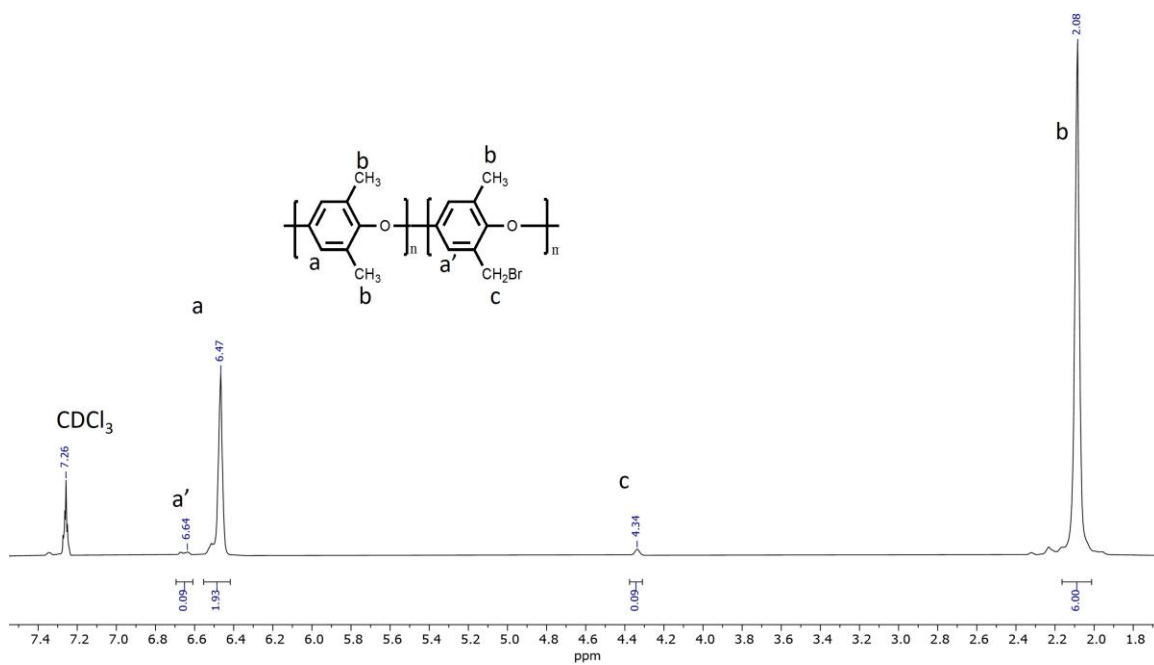


Figure 3.5: ^1H NMR spectrum indicating successful synthesis of Br-PPO.

Table 3.4: Characteristics of Br-PPO macroinitiator.

Sample ^a	M_n (kDa)	M_w (kDa)	Đ	Rxn time (min)	# of Br Sites
4.5% Br	16.7	37.7	2.25	60	8
10% Br	13.8	35.7	2.59	75	15
28% Br	17.6	45.5	2.56	90	27
59% Br	19.8	47.3	2.39	120	79

^a Bromination level of the PPO backbone

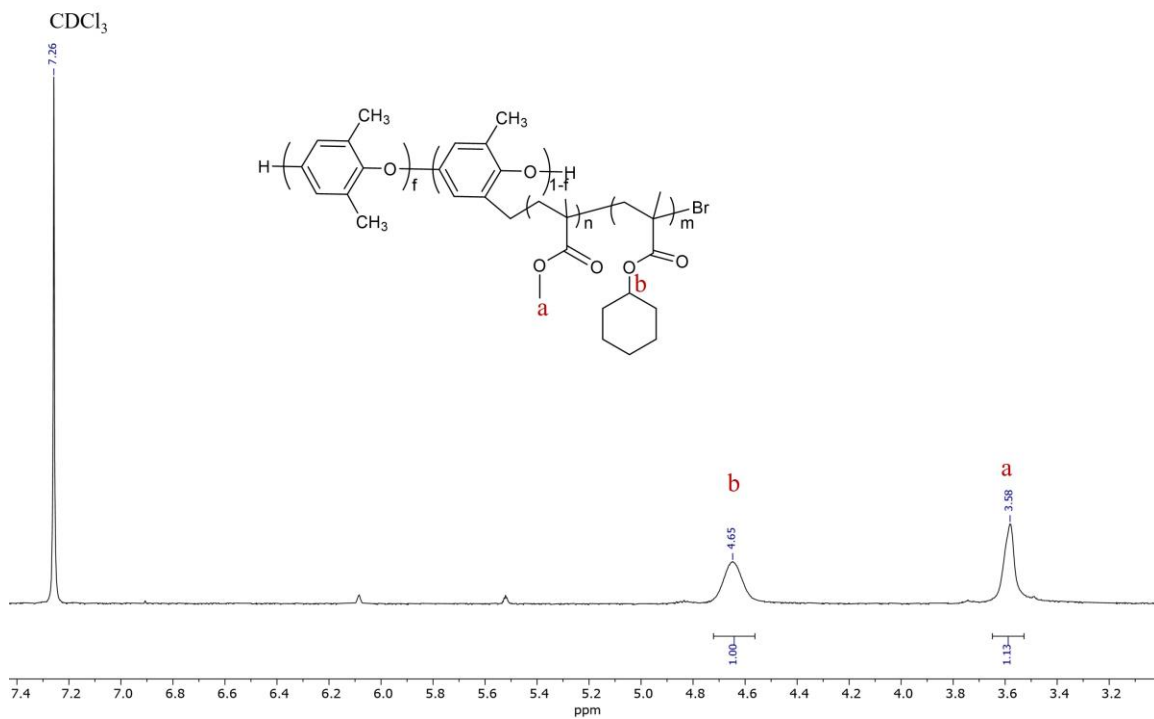


Figure 3.6: ^1H NMR spectrum of PrC brush-like copolymer synthesized from a 28% Br-PPO as a macroinitiator. The peak at 3.58 ppm corresponds to the methyl ester of MMA, whereas the peak at 4.56 ppm corresponds to the bridgehead proton of the CHMA.

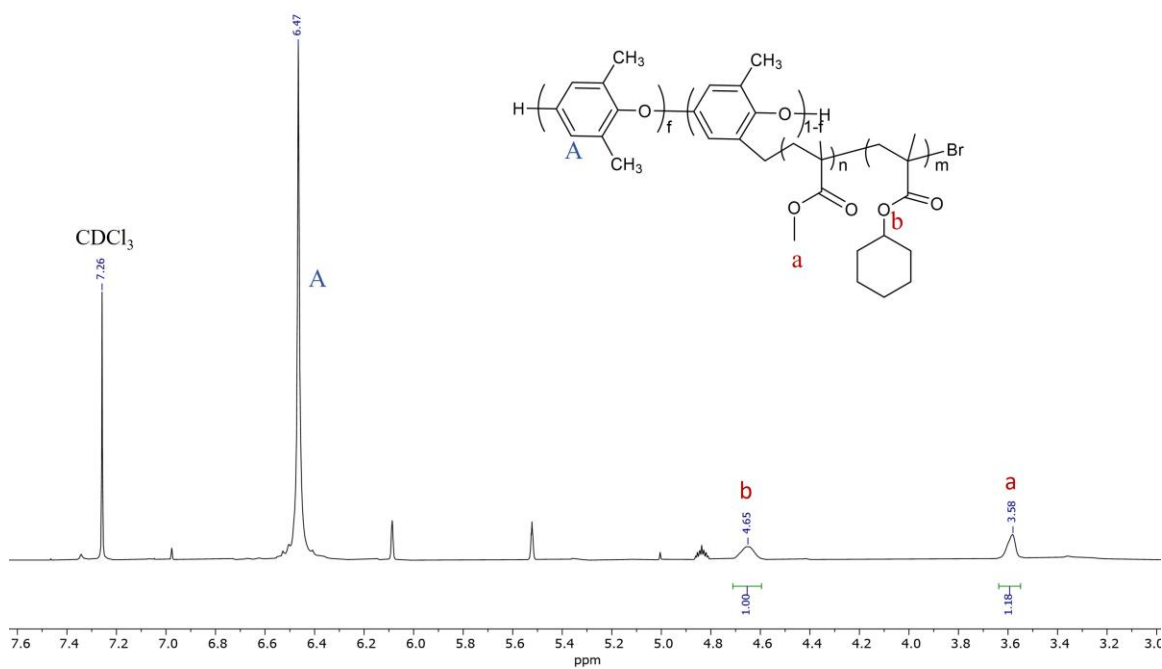


Figure 3.7: ^1H NMR spectrum of PrC brush-like copolymer utilizing 4.5% Br-PPO as a macroinitiator. The peak at 3.58 ppm corresponds to the methyl ester of MMA whereas peak at 4.56 ppm corresponds to the bridgehead proton of the CHMA. The peak at 6.47 ppm corresponds to aromatic proton labeled “A” within the structure.

observed, and GPC shows $M_n = 18.8$ kDa. These two pieces of evidence indicate that the brushes are of very low molecular weight. I attempted a variety of syntheses at various $[M]/[I]$, as reflected in **Table 3.5**, and the results seem to follow a trend: syntheses that use Br-PPOs having a low number of bromination sites resulted in very low activation of the ligand system, thus limiting the formation of side chains. On the other hand, Br-PPO macroinitiators with a higher number of bromination sites resulted in crosslinking between the side chains and/or the macroinitiator (PPO backbone) itself. Many different trials were performed, adjusting parameters such as solvent type, temperature, polymerization time and ligand to no avail. A few of these reactions are summarized in **Table 3.5**. To counteract the problems seen with this grafting from approach, a grafting onto method based on click chemistry is being explored. Preliminary studies involving the synthesis of an alkyne-terminated initiator that would be used to synthesize side chains via ATRP is presented in **Figure 3.8**. In order to attach side chains to the backbone, Br-PPO was modified to create an azide-functionalized PPO. Alkyne-terminated PrC copolymer side chains were polymerized by ATRP at $[M]/[I]$ of 100:1, which targets side chains of 14.6kDa. The ^1H NMR of the copolymer product is presented in **Figure 3.9**, where a composition of 72:28 CHMA:MMA was observed for the alkyne-terminated PrC. In addition, the ^1H NMR spectrum shows the preservation of the alkynyl proton, which is seen at 2.26 ppm. The molecular weight of the copolymer was measured to be $M_n = 15.4$ kDa and the elution trace is shown in **Figure 3.10**. The unimodal peak indicates a well-controlled polymerization of the alkyne terminated PrC at the 0.7 molar target CHMA composition. This reaction was replicated to synthesize copolymers with M_n of 12.7 and 9.3kDa. A click chemistry reaction between the azide-

Table 3.5: Analysis of comb-like copolymers utilizing PPOs of various bromination percentages.

Sample	[M]/[I]^a	%Br	M_n (kDa)	M_w (kDa)	Đ	Solvent	Rxn Time (h)
Trial 1	[100]:[1]	28	3.707×10 ³	3.73×10 ³	1.21	Benzene	6
Trial 2	[50]:[1]	28	3.35×10 ³	5.01×10 ³	1.49	Benzene	6
Trial 3	[100]:[1]	4.5	19.0	26.3	1.41	Benzene	6
Trial 4	[20]:[1]	4.5	18.8	25.7	1.37	Benzene	6

^a Calculated based on total CHMA and MMA amounts and total number of Br sites on Br-PPO. [Ligand]: [Catalyst] for all trials set at 1:1 ratio with respect to [M]:[I] ratio.

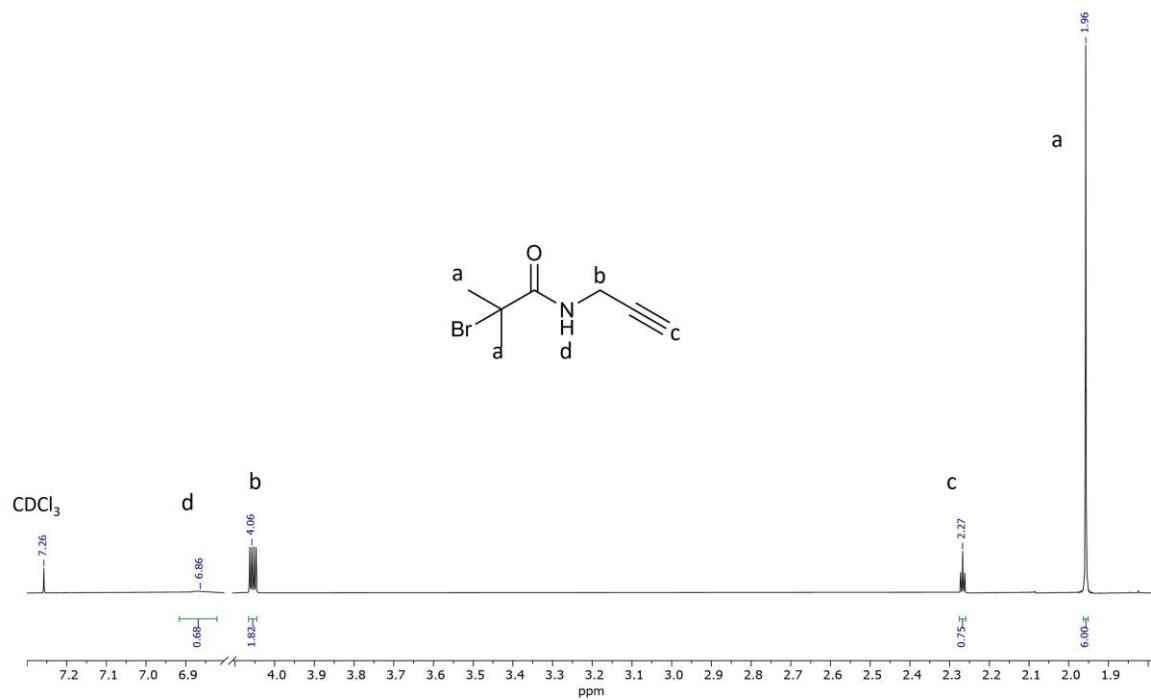


Figure 3.8: ¹H NMR of 2-bromo-2-methyl-N-(prop-2-yn-1-yl) propanamide (BMPP), which is an initiator used to synthesize alkyne-terminated PrC copolymer side chain.

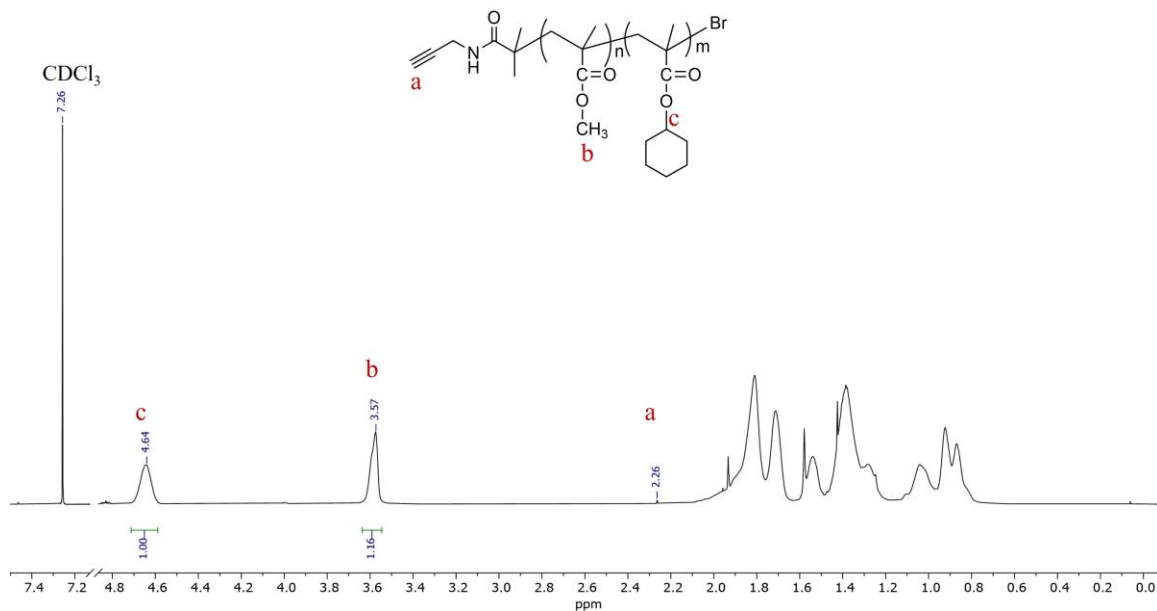


Figure 3.9: ¹H NMR spectrum of the alkyne-terminated PrC utilizing BMPP as an initiator for the successful synthesis of 15.4 kDa side chains. The peak at 2.26 ppm confirms the presence of the terminal alkyne used for click reactions between azide groups on the azide-functionalized PPO.

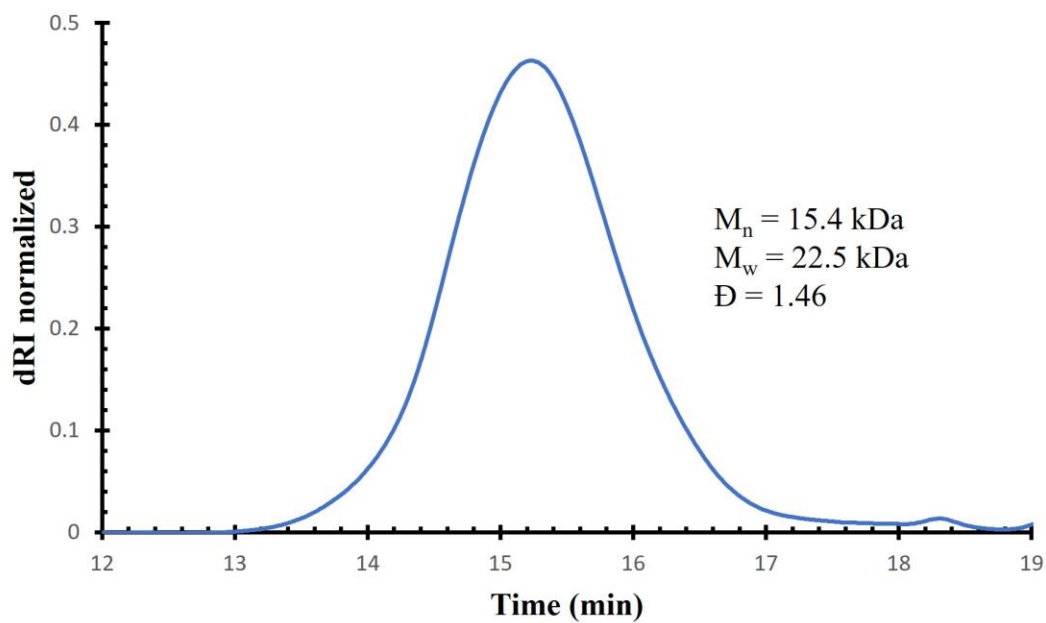


Figure 3.10: GPC chromatogram indicating successful synthesis of alkyene-terminated PrC copolymer side chains.

functionalized PPO, PPO-N₃, and the alkyene-terminated PrC copolymers is to be performed. This strategy is expected to enable access to brush copolymers.

CHAPTER FOUR

CONCLUSIONS AND RECOMMENDATIONS

In this thesis, synthetic strategies for the preparation of linear and branched PrC copolymers via two different controlled radical polymerization techniques were introduced. For the synthesis of linear PrCs, a CHMA composition of 0.7 was chosen due to the highest attractive interaction with the PS blocks (domains) of TPE. I was also able to successfully synthesize linear PrC copolymers having molecular weights ranging from 2.8 kDa to 65.5 kDa, as shown in **Table 3.1**, and these were subsequently incorporated into a TPE matrix to assess impact on creep behavior and morphology via Small Angle X-Ray Scattering (SAXS). A route for the synthesis of branched copolymers utilizing Br-PPO as a macroinitiator via ATRP was observed to be problematic, lacking reproducibility either due to slow activation of the benzylic halide groups at lower bromination level or significant crosslinking at modest to high bromination levels. If this polymerization route is to be utilized again using Br-PPO as a macroinitiator, more systematic studies utilizing different pairs of monomers will be needed to identify workable ATRP conditions. I also explored a grafting onto approach to create PrC-modified PPOs. This was accomplished by initially synthesizing an alkyne-terminated initiator, which was then subsequently utilized to synthesize PrC copolymer side chains at various molecular weights via ATRP. Future work entails successful click chemistry synthesis utilizing the azide-functionalized PPO along with alkyne-terminated PrC side chains along with in-depth, follow-on studies to understand the stability of the brushes, the triazole ring under annealing conditions, and investigating the effect of branched PrC

copolymers on the mechanical and morphological properties of SEBS-type TPEs.

LIST OF REFERENCES

1. Das, S.; Cox, D. F.; Wilkes, G. L.; Klinedinst, D. B.; Yilgor, I.; Yilgor, E.; Beyer, F. L., Effect of Symmetry and H-bond Strength of Hard Segments on the Structure-Property Relationships of Segmented, Nonchain Extended Polyurethanes and Polyureas. *Journal of Macromolecular Science, Part B* **2007**, *46* (5), 853-875.
2. Fredrickson, G. H.; Helfand, E., Fluctuation Effects in the Theory of Microphase Separation in Block Copolymers. *The Journal of Chemical Physics* **1987**, *87* (1), 697-705.
3. Sunday, D. F.; Hannon, A. F.; Tein, S.; Kline, R. J., Thermodynamic and Morphological Behavior of Block Copolymer Blends with Thermal Polymer Additives. *Macromolecules* **2016**, *49* (13), 4898-4908.
4. Bates, F. S.; Fredrickson, G. H.; Hucul, D.; Hahn, S. F., PCHE-based Pentablock Copolymers: Evolution of a New Plastic. *AIChE Journal* **2001**, *47* (4), 762-765.
5. Nishimoto, M.; Keskkula, H.; Paul, D. R., Blends of Poly(styrene-co-acrylonitrile) and Methyl Methacrylate based Copolymers. *Macromolecules* **1990**, *23* (15), 3633-3639.
6. Madathil, K.; Upadhyay, B.; Ledford, W. K.; Kilbey, S. M., II; Stein, G. E., Structure-Property Relations of Triblock Copolymer Thermoplastics with Interaction-Tuned Polymer Additives. *Macromolecules* **2023**, *56* (17), 7102-7112.
7. Lynd, N. A.; Oyerokun, F. T.; O'Donoghue, D. L.; Handlin, D. L.; Fredrickson, G. H., Design of Soft and Strong Thermoplastic Elastomers Based on Nonlinear Block Copolymer Architectures Using Self-Consistent-Field Theory. *Macromolecules* **2010**, *43* (7), 3479-3486.
8. Drobny, J. G., *Handbook of Thermoplastic Elastomers*. Elsevier Science & Technology Books: Norwich, UNITED STATES, 2014.
9. Jiang, F.; Wang, Z.; Qiao, Y.; Wang, Z.; Tang, C., A Novel Architecture Toward Third-Generation Thermoplastic Elastomers by a Grafting Strategy. *Macromolecules* **2013**, *46* (12), 4772-4780.
10. Shi, W.; Lynd, N. A.; Montarnal, D.; Luo, Y.; Fredrickson, G. H.; Kramer, E. J.; Ntaras, C.; Avgeropoulos, A.; Hexemer, A., Toward Strong Thermoplastic Elastomers with Asymmetric Mikroarm Block Copolymer Architectures. *Macromolecules* **2014**, *47* (6), 2037-2043.
11. Lilaonitkul, A.; Cooper, S. L. Properties of Polyether-Polyester Thermoplastic Elastomers. *Rubber Chemistry and Technology* **1977**, *50* (1), 1-23.
12. Elabd, Y. A.; Napadensky, E.; Walker, C. W.; Winey, K. I., Transport Properties of Sulfonated Poly(styrene-b-isobutylene-b-styrene) Triblock Copolymers at High Ion-Exchange Capacities. *Macromolecules* **2006**, *39* (1), 399-407.
13. Mori, Y.; Lim, L. S.; Bates, F. S., Consequences of Molecular Bridging in Lamellae-Forming Triblock/Pentablock Copolymer Blends. *Macromolecules* **2003**, *36* (26), 9879-9888.
14. Nasiri, M.; Saxon, D. J.; Reineke, T. M., Enhanced Mechanical and Adhesion Properties in Sustainable Triblock Copolymers via Non-Covalent Interactions. *Macromolecules* **2018**, *51* (7), 2456-2465.
15. Matsen, M. W.; Thompson, R. B., Equilibrium Behavior of Symmetric ABA Triblock Copolymer Melts. *The Journal of Chemical Physics* **1999**, *111* (15), 7139-7146.
16. Zheng, W.; Wang, Z.-G., Morphology of ABC Triblock Copolymers. *Macromolecules* **1995**, *28* (21), 7215-7223.
17. Aggarwal, S. L., Structure and Properties of Block Polymers and Multiphase Polymer Systems: An Overview of Present Status and Future Potential. *Polymer* **1976**, *17* (11), 938-956.
18. Laurer, J. H.; Hajduk, D. A.; Fung, J. C.; Sedat, J. W.; Smith, S. D.; Gruner, S. M.; Agard, D. A.; Spontak, R. J., Microstructural Analysis of a Cubic Bicontinuous Morphology in a Neat SIS Triblock Copolymer. *Macromolecules* **1997**, *30* (13), 3938-3941.

19. Kwak, Y.; Matyjaszewski, K., ARGET ATRP of Methyl Methacrylate in the Presence of Nitrogen-based Ligands as Reducing Agents. *Polymer International* **2009**, *58* (3), 242-247.
20. Matyjaszewski, K.; Ziegler, M. J.; Arehart, S. V.; Greszta, D.; Pakula, T., Gradient Copolymers by Atom Transfer Radical Copolymerization. *Journal of Physical Organic Chemistry* **2000**, *13* (12), 775-786.
21. Liang, M.; Jhuang, Y.-J.; Zhang, C.-F.; Tsai, W.-J.; Feng, H.-C., Synthesis and Characterization of Poly(phenylene oxide) Graft Copolymers by Atom Transfer Radical Polymerizations. *European Polymer Journal* **2009**, *45* (8), 2348-2357.
22. Vogt, A. P.; Sumerlin, B. S., An Efficient Route to Macromonomers via ATRP and Click Chemistry. *Macromolecules* **2006**, *39* (16), 5286-5292.
23. Ding, L.; Huang, Y.; Zhang, Y.; Deng, J.; Yang, W., Optically Active Amphiphilic Polymer Brushes Based on Helical Polyacetylenes: Preparation and Self-Assembly into Core/Shell Particles. *Macromolecules* **2011**, *44* (4), 736-743.
24. Hashimoto, T.; Kimishima, K.; Hasegawa, H., Self-assembly and Patterns in Binary Mixtures of SI block Copolymer and PPO. *Macromolecules* **1991**, *24* (20), 5704-5712.
25. Zhang, L. In *Thin-film Block Copolymers (BCPs) Self-assembly as Versatile Patterning Scheme for Functional Nanomaterials*, **2018**.
26. Davis, R. L.; Jayaraman, S.; Chaikin, P. M.; Register, R. A., Creating Controlled Thickness Gradients in Polymer Thin Films via Flowcoating. *Langmuir* **2014**, *30* (19), 5637-5644.
27. Tsige, M.; Grest, G. S., Solvent Evaporation and Interdiffusion in Polymer Films. *Journal of Physics: Condensed Matter* **2005**, *17* (49), S4119-S4132.
28. Zhang, J.; Wu, P., Grafting Polymers from Poly(2,6-dimethyl-1,4-phenylene oxide) as New Thermoplastics. *Macromolecular Chemistry and Physics* **2017**, *218* (11), 1700023.
29. Semerci, E.; Bedri, T. E.; Kizilcan, N., Preparation of Thermal Conductive Poly(methyl methacrylate)/Silicon Nitride Nanocomposites via Click Chemistry. *Polymer* **2021**, *212*, 123285.
30. Lutz, J.-F.; Börner, H. G.; Weichenhan, K., Combining Atom Transfer Radical Polymerization and Click Chemistry: A Versatile Method for the Preparation of End-Functional Polymers. *Macromolecular Rapid Communications* **2005**, *26* (7), 514-518.
31. Aden, B.; Kite, C. M.; Hopkins, B. W.; Zetterberg, A.; Lokitz, B. S.; Ankner, J. F.; Kilbey, S. M., II, Assessing Chemical Transformation of Reactive, Interfacial Thin Films Made of End-Tethered Poly(2-vinyl-4,4-dimethyl azlactone) (PVDMA) Chains. *Macromolecules* **2017**, *50* (2), 618-630.

VITA

Originally from Nepal, Bishal Upadhyay grew up along the foothills of the Himalayas, where he completed schooling through most of his high school years. He moved to the United States in 2012 and, after finishing high school, he pursued his bachelor's degree at the University of Southern Mississippi, where he studied polymer science. As an undergraduate, he did research in the group of Prof. Sarah Morgan. During his work in the Morgan research group, he was able to shadow different graduate students and learned from their research work, which inspired his interests in polymer synthesis and their uses. Therefore, he decided to pursue a Master of Science degree in chemistry at the University of Tennessee, Knoxville. His research interest includes copolymer synthesis utilizing various controlled and free radical polymerization techniques and their subsequent analysis. After graduation, he plans to begin professional practice as a chemist. He is very grateful for the constant support and help of his advisor, his friends within and outside of his research lab throughout his graduate studies, and his mother back home, who has always pushed him to move forward.